# Malleable conformation of the elastic PEVK segment of titin: non-co-operative interconversion of polyproline II helix, $\beta$-turn and unordered structures

Kan MA and Kuan WANG[1]

Muscle Proteomics and Nanotechnology Section, Laboratory of Muscle Biology, National Institute of Arthritis and Musculoskeletal and Skin Diseases, National Institutes of Health, Bethesda, MD 20892, U.S.A.

To understand the structural basis of molecular elasticity and protein interaction of the elastic PEVK (Pro-Glu-Val-Lys) segment of the giant muscle protein titin, we carried out a detailed analysis of a representative PEVK module and a 16-module PEVK protein under various environmental conditions. Three conformational states, polyproline II (PPII) helix, $\beta$-turn and unordered coil were identified by CD and NMR. These motifs interconvert without long-range co-operativity. As a general trend, the relative content of PPII increases with lower temperature and higher polarity, $\beta$-turn increases with lower temperature and lower polarity, and unordered coil increases with higher temperature and higher polarity. NMR studies demonstrate that *trans*-proline residues are the predominant form at room temperature (22 °C), with little *trans*-to-*cis* isomerization below 35 °C. Ionic strength affects salt bridges between charged side chains, but not the backbone conformation. We conclude that titin PEVK conformation is malleable and responds to subtle environmental changes without co-operativity. This gradual conformational transition may represent a regulatory mechanism for fine-tuning protein interactions and elasticity.

Key words: circular dichroism (CD), elastic protein, nuclear magnetic resonance (NMR), polyproline II helix-coil (PhC) motif, titin, *trans*-to-*cis*-proline isomerization.

## INTRODUCTION

Titin represents a family of giant elastic proteins (3–4 MDa) found mainly in skeletal and cardiac muscles [1,2], and its gene is notable for encoding the largest protein in the entire human genome [3,4]. Its multifaceted functions include the assembly of the muscle sarcomere, the maintenance of sarcomere symmetry and integrity and the generation of passive tension (reviewed in [5,6]). Titin accomplishes these functions by spanning half of the muscle sarcomere length and anchoring the myosin thick filament from the M-line to the Z-line. In the I-band region, where titin extends during passive force development, titin is composed of serial-linked motifs of three types: (i) the folded 100-residue modular repeats of immunoglobin (Ig) or fibronectin (Fn3) domains, (ii) the N2-A or N2-B insert, and (iii) a unique PEVK motif that consists of 70 % of proline, glutamate, valine, and lysine residues [7,8]. The extension of this unique segment accompanies the rise in passive tension when resting muscle is stretched moderately, while maintaining the overlap of the actin and myosin filaments [5,9,10]. However, the exact nature of both the structure and elasticity of the PEVK segment is still unresolved.

The PEVK segment is also a major site for potential protein interaction. The segment appears to be involved in interfilament adhesion with thin filaments via its interaction with actin and nebulin in a calcium/S100-sensitive manner [11]. Cardiac PEVK also binds S100 directly [12]. Our recent search for SH3 (Src-homology 3)-binding motifs in titin isoforms revealed a surprising enrichment of class I and class II SH3 binding motifs in the PEVK regions [13,14]. More significantly, biophysical studies revealed the direct interaction of a nebulin SH3 domain with titin PEVK peptides at the central PPII (polyproline II) helix of PEVK modules, suggesting the intriguing possibility that titin PEVK is an extended signalling domain containing multiple SH3-binding sites in tandem repeats. These proline-rich regions may thus have a scaffolding role in the signalling pathway during muscle assembly [13].

Conformational studies of PEVK modules are essential for our understanding of the structural basis of their protein–protein interactions and elasticity. On the assumption that the PEVK segment is a random coil or a permanently unfolded linear polypeptide [8,9,15], it is often stated that PEVK resists stretching by maximizing entropy and behaving as a worm-like chain (WLC) [16–18]. Evidence of the presence of stable and regular structural features in the PEVK segment is emerging. We reported that the PEVK of human foetal skeletal muscle titin is modular and consists of tandem repeats of a fundamental PEVK module that average 28 residues [11]. Independent analysis of the PEVK sequences by Greaser [17] corroborated our conclusions and revealed another repeating motif: a glutamate-rich acidic motif of variable length [17]. Other PEVK-like proline-rich repeats in titin or related proteins include two large PEVK domains in D-titin from *Drosophila* [19], 70-residue repeats (ten modules) in PEVK-1 and 17-residue repeats (45 modules) in PEVK-2 from invertebrate connectin [20], 39-residue repeats (57 modules) in PEVT/K from *Caenorhabditis elegans* titins [21], and 65-residue repeats (22 modules) from a MLCK (myosin light chain kinase)-like giant protein from *Drosophila* [22].

Abbreviations used: CCA, Convex Constraint Analysis; NOE, nuclear Overhauser effect; PEVK, a titin segment that consists mainly of proline, glutamate, valine and lysine; PhC, PPII helix-coil; PPII, polyproline II; PR, a 28-mer sequence module of PEVK corresponding to human PEVK exon 172, $P^{1}$EPPKEVVPEKKAPVAPPKKPEVPPVKV$^{28}$; ROESY, rotating frame NOESY; SH3, Src-homology 3; TFE, trifluoroethanol; TP1, expressed PEVK segment of human foetal skeletal titin exons 161–164, 166–177, 180–181.

[1] To whom correspondence should be addressed (e-mail wangk@exchange.nih.gov).

Conformational and hydrodynamic studies of an expressed 16-PEVK module (473 residues) protein fragment of human foetal titin, designated TP1, have shown that TP1 is an open and flexible chain with stable structural folds [11]. Conformational studies by CD indicated the probable presence of PPII type left-handed helices in TP1. Further examination of this and other PEVK sequences of titin revealed the presence of numerous PXXP (Pro-Xaa-Xaa-Pro) motifs (e.g. PVAP) that are frequently found in PPII-like left-handed helices. These observations suggest that PPII may indeed be a major structural motif of PEVK in titin.

Our recent two-dimensional NMR and CD studies of synthetic peptides of one representative 28-residue PEVK module for human foetal titin ($P^{1}$EPPKEVVPEKKAPVAPPKKPEVPPVKV$^{28}$, designated PR) as well as three subfragments (PR1, $K^{-2}$VPEPPKEVVPE$^{10}$; PR2, $V^{8}$PEKKAPVAPPK$^{19}$; PR3: $K^{20}$PEVPPVKV$^{28}$) revealed the presence of three PPII helices that are three residues per left-handed turn with $\phi$ and $\psi$ angles restricted to regions $-78$ and $+146$ respectively [23]. Structural determinations indicated the presence of three short stretches of PPII helices of four, five and six residues that were interspersed with unordered and presumably flexible spacer regions to give one 'PPII helix-coil' or 'PhC' motif for roughly every ten residues. These peptides also displayed the characteristic PPII CD spectra: i.e. positive peak or negative shoulder band at 223 nm, negative CD band near 200 nm, and biphasic thermal titration curves that reflect varied stability of these PPII helices. We have proposed that this PhC motif is a fundamental feature, and that the number, length, stability and distribution of PPII are important in the understanding of the elasticity and protein interactions of the PEVK region of titin [23].

In the present study, we present a detailed analysis of the conformational states of these peptides and their interconversion under various environmental conditions, such as temperature, ionic strength and solvent polarity. Since the PPII helices are found in PXPP, PXXPP and XPXXPP sequences, the possible roles of *trans*/*cis*-proline isomerization in the conformational stability is of obvious interest. Our studies indicate that three conformational states are resolvable by quantitative CD analysis: PPII helix, $\beta$-turn and unordered coil. These motifs interconvert and, as a general trend, the relative content of PPII increases with lower temperature and higher polarity, $\beta$-turn increases with lower temperature and lower polarity, and unordered coil increases with higher temperature and higher polarity. NMR studies demonstrate the expected coexistence of the *trans*- and *cis*-proline conformers in these peptides, with *trans*-proline being the predominant form. However, little *trans*-to-*cis* isomerization takes place when the temperature is elevated from 2 to 35 °C. CD and NMR analysis indicate the presence of type I $\beta$-turns within the sequence of the PEVK module ($K^{5}$EVVPEK$^{11}$) in 80 % trifluoroethanol (TFE). We conclude that the titin PEVK segment is malleable conformationally, and environmental conditions easily tip the balance among three states, without involving proline *trans*-to-*cis* isomerization.

## MATERIALS AND METHODS

### Peptide synthesis and TP1 expression

The peptides used in this study, one full PEVK module (PR, exon 172) and three subfragments (PR1, PR2 and PR3), were synthesized and purified before use as described previously [23]. TP1 (exons 161–164, 166–177, 180–181), a 51 kDa (473 residues) human foetal titin PEVK fragment, was expressed and purified from *Escherichia coli* host cells transformed with pET3d *Hin*fI plasmid containing a 1.4 kb open reading frame derived from hfT11 (human foetal titin fragment) cDNA (GenBank® accession number AF321609) as described previously [11]. TP1 concentration was determined spectrophotometrically based on its absorption coefficient ($A_{280}$) of 0.025 for 1 mg/ml. Polyproline ($M_r = 5000$; Sigma) was used without further purification.

### Search of conformational motifs

A search for conformational motifs on the human titin gene exons that encode PEVK segments (GenBank® accession number AJ277892) was performed with MacVector (version 6.5.3) for PXXP, PXPP, XPXXPP, VPE, KEVV and VPEK. Alignment of PEVK module sequences was performed with ClustalW.

### CD and deconvolution

All spectra were obtained with a Jasco spectropolarimeter, model J-715, equipped with the standard data analysis program (Jasco, Tokyo, Japan). The temperature was controlled with a Peltier-type temperature-control system, model PTC-348WI (Jasco). The synthetic PEVK peptides were soluble in aqueous solutions and in TFE. All solutions contained 10 mM potassium phosphate and the pH was adjusted to the desired level at room temperature (22 °C).

A quartz cell with a 0.1 cm path length was used, and spectra were recorded with a 1.0 nm bandwidth and resolution of 0.1 nm over the wavelength range 180–250 nm. A mean was taken from four scans for both sample and solvent to improve the signal/noise ratio, and all spectra were obtained by subtracting buffer spectra.

The CD data gave a linear correlation between peptide concentration (over a 30-fold range from 20 to 600 $\mu$M) and ellipticity at both 201 nm ($\pi$-$\pi^*$ transition) and 222 nm (n-$\pi^*$ transition) (results not shown), indicating that the PEVK peptide used in the present study was either monomeric or, even if aggregated at higher concentration, did not affect the conformations that contributed to CD. The line width of NMR signals did not broaden when the peptides were dissolved in 80 % TFE at mM concentrations, indicating that no aggregation occurred in the TFE solution.

The CD spectra of PR peptides were recorded in aqueous solutions at different pH values at 2, 22 and 60 °C. The CD spectra remained essentially unchanged within the pH range 4.6–10.2 at 2 and 60 °C, and pH range 2.6–10.2 at 22 °C. When the temperature was raised from 2 to 70 °C, the pH of 10 mM potassium phosphate varied from pH 7.2 to 7.0. Since pH had little effect, changes of the CD spectra were attributed exclusively to temperature.

Secondary-structure analysis by deconvolution of CD spectra was performed with the CCA (Convex Constraint Analysis) program [24,25] kindly supplied by Professor Norma Greenfield of Robert Wood Johnson Medical School (Piscataway, NJ, U.S.A.). This was deemed ideal for examining the CD spectra of these small peptides with a limited number of conformational motifs [26]. Other programs such as Selcon II and III [27–29] were more appropriate for much larger proteins with a multitude of structural motifs.

Two independent sets of CD spectra (180–250 nm) were deconvoluted to determine the residual ellipticity and a minimal set of component motifs. The first one consisted of 15 spectra (five spectra per peptide) collected at 2, 20, 40, 60 and 80 °C in aqueous solution. The second set included 12 spectra (four spectra per peptide) obtained in 0, 40, 80 and 100 % TFE at 2 °C. To determine the optimal set of components, spectra of PR1, PR2 and PR3 at various temperatures or TFE concentrations were first subjected to two-, three-, four-, five- and six-component fits, and evaluated based on the criterion of the appearance of two or more curves with similar features as an indication of overestimation of the number of components. Three components were found to be

minimal, and were used to deconvolute PR spectra. The relative molar proportion of the resulting three CCA components in PR at different temperatures or TFE concentration was estimated by the Lincomb program [25].

### NMR spectroscopy

NMR spectroscopy was performed essentially as described previously [23]. Briefly, the peptides were freeze-dried before being rehydrated in $H_2O/^2H_2O$ (9:1 molar ratio) or $^2H_2O$, containing 10 mM sodium phosphate buffer (pH 6.9) and TSP [3-(trimethylsilyl)-propionate-2,2,3,3-$d_4$] (0.05 mM), which serves as an internal chemical shift reference at 0 p.p.m. Final concentrations of 4–5 mM peptide solutions were attained. For measurements in TFE, deuterated TFE was added to a concentration of 80 % in 10 mM sodium phosphate. The samples were centrifuged at 16 000 ***g*** for 30 min to remove any aggregates. All $^1$H NMR spectra at 5, 15, 25, 35 and 80 °C were obtained at 600 MHz using a Varian UnityPlus-600 spectrometer. The NMR data were transferred to SGI (Silicon Graphics, Inc., Mountain View, CA, U.S.A.) computer workstations and processed using the FELIX program (FELIX 97.0; Biosym, Inc., San Diego, CA, U.S.A.). Two-dimensional TOCSY [30] and H–H ROESY (rotating frame NOESY) [31] were used to study the conformation change of PEVK peptides.

## RESULTS AND DISCUSSION

The present study was initiated as a systematic study to pursue the factors that may cause conformational transitions of PPII-coil motifs in the PEVK modules of the elastic segments of titin. We report significant effects of temperature, ionic strength, urea and TFE on the conformation of PEVK peptides/TP1 as monitored by CD and NMR.

### Evidence of three conformational states: PPII, $\beta$-turn and unordered coil

As a reference for PPII conformation, the CD spectra of polyproline, which adopts an extended PPII helix structure in aqueous solutions, were first measured. It exhibited a weak positive band at 229 nm (n-$\pi^*$) and a strong negative band at 206 nm ($\pi$-$\pi^*$) [23]. Upon heating, both bands decreased in magnitude with an isodichroic point at 215 nm [11].

Temperature change significantly altered the CD spectra of PR1, PR2, PR3 and PR (Figures 1C, 1E, 1G and 1I). As a general trend, less intense negative and positive bands and a red shifting of the negative band were observed with increasing temperatures (between the range of 2 to 80 °C). The presence of isodichroic points for PR1, PR2, PR3 and PR around 211 nm indicated equilibrium between two states [23]. For quantitative analysis, CCA was selected as the most suitable program for this set of small peptides because each set of CD spectra (i.e. temperature, pH) could be resolved into a minimal number of components necessary to reconstruct all the observed CD spectra.

Three components were sufficient to reconstruct the spectra within the experimental error (Figure 1A). Component I had a strong negative maximum at 199 nm and a weak positive band near 224 nm, which was assigned to the PPII conformation [23,32,33]. Component II had a less intense negative band at 201 nm and a negative shoulder at 220 nm, which has been previously shown to be a prominent feature of the CD of an unordered conformation [34]. Component III exhibited a broad weak negative band at 213 nm and a weak positive band around 189 nm, reminiscent of the spectra of type I $\beta$-turn conformation with two negative bands at 208 and 215 nm, and one positive band near 188 nm [34,35].

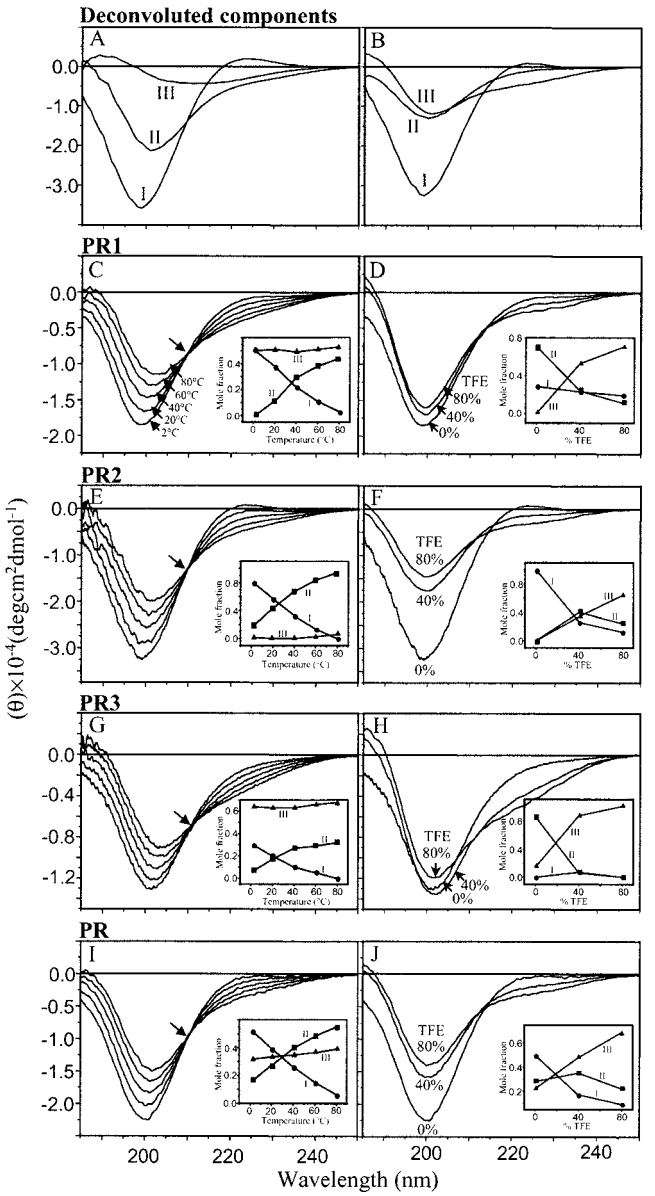


**Figure 1 Three conformational states of PEVK peptides at varying temperatures and TFE concentrations**

Left-hand panels: thermal titration (2–80 °C) of PEVK peptides by CD. (**A**) Three conformational components I, II and III resulting from CCA deconvolution of all CD spectra in 10 mM potassium phosphate, pH 7.0. (**C**) PR1, 0.35 mg/ml. (**E**) PR2, 0.4 mg/ml. (**G**) PR3, 0.46 mg/ml. (**I**) PR, 0.15 mg/ml. Insets show the changes in the relative content (mole fractions) of conformational states of each peptide at 2, 20, 40, 60 and 80 °C. (●, ■, ▲ for component I, II and III respectively). Small arrows indicate the isodichroic points. Right-hand panels, TFE titration of PEVK peptides by CD. (**B**) Three conformational states resulting from CCA deconvolution of all spectra in 0 %, 40 % and 80 % (v/v) TFE, 10 mM potassium phosphate, pH 7.0. (**D**) PR1, 0.26 mg/ml. (**F**) PR2, 0.26 mg/ml. (**H**) PR3, 0.31 mg/ml. (**J**) PR, 0.15 mg/ml. Insets reveal the changes in the relative contents (mole fractions) of conformational states of each peptide in TFE (●, ■, ▲ for component I, II and III respectively).

Based on these observations, component III was assigned as a $\beta$-turn, with a small molar ellipticity.

The relative contents of the three components at different temperatures indicated that the PPII conformation decreases with higher temperatures for all peptides. PR contained 52 % PPII at 2 °C and only 6 % PPII at 80 °C (Figure 1I, inset). Turn conformation (component III) remained nearly constant (Figure 1I, inset)

and unordered structure was increased from 16 % at 2 °C to 55 % at 80 °C, indicating an interconversion of two states. A similar trend was also observed for the 16-module PEVK protein, TP1 [11].

Overall, PR2 contained more PPII than the other three peptides at a given temperature with a decreasing order of PR2 > PR > PR1 > PR3. The content of PPII within all peptides decreased gradually with increased temperature (2–80 °C) (Figures 1C, 1E, 1G and 1I, insets). It should be noted that the CCA program is useful mostly in indicating the trend of the conformational change rather than the absolute value of the conformation.

### TFE induces $\beta$-turn

Since the thermal titration data suggested the presence of a $\beta$-turn structure in PEVK peptides, the influence of TFE, which tended to promote secondary conformation transition [36], was then investigated. The CD spectra for PR1, PR2, PR3 and PR in different concentrations of TFE did not display isodichroic points, indicating the coexistence of multiple conformations (Figures 1D, 1F, 1H and 1J). The strong negative peak at 200 nm shifted slightly to 201 nm and the negative ellipticity around 222 nm increased with higher concentrations of TFE. A difference spectrum between 0 and 80 % TFE at room temperature (results not shown) appeared to correspond to a type I $\beta$-turn spectrum, as classified by Woody [34], with a minimum at approx. 225 nm and a maximum at approx. 190 nm. As temperature increased, less $\beta$-turn structure was present, as monitored by difference spectra at 189 and 224 nm (results not shown).

Analysis of these spectra with CCA (Figure 1B) yielded the same three components from the temperature series (Figure 1A). Turn structure increased with higher concentrations of TFE, whereas PPII and coil both decreased (Figures 1D, 1F, 1H and 1J, insets).

The subclass and locations of $\beta$-turns were elucidated by NMR. The most notable changes in the ROESY spectra in 80 % TFE were the connectivity of $\alpha$H-NH(i, i + 2) and NH-NH(i, i + 1) (Figures 2A and 2B) that were absent in aqueous solution [23]. Specifically, NOEs (nuclear Overhauser effects) between the amide proton of Lys$^5$-Glu$^6$, Glu$^6$-Val$^7$, Val$^7$-Val$^8$, Glu$^{10}$-Lys$^{11}$ and Lys$^{11}$-Lys$^{12}$ revealed newly formed $\beta$-turns in the region of K$^5$EVVPEKK$^{12}$ (Figure 2B), which were unordered coils in aqueous solution [23]. A closer examination of NOEs and $^3J_{\alpha N}$ coupling constants suggested the presence of type I $\beta$-turns at K$^5$EVV$^8$ and V$^8$PEK$^{11}$. The NOE connectivity between the $\delta$H of Pro$^9$ and the NH of Glu$^{10}$ ruled out type II $\beta$-turns because the $d_{\delta N}$ distance for this type was about 5.6 Å (1 Å = 0.1 nm) and was therefore unobservable by NMR. Furthermore, the large $^3J_{\alpha N}$ coupling constants for Val$^7$ (8.6 Hz) and Glu$^{10}$ (7.8 Hz) ruled out type III $\beta$-turns, whose calculated $^3J_{\alpha N}$ value was 4.2 Hz (Figure 2C). At first glance, the medium-to-weak NOEs between the $\alpha$H of Glu$^6$ and the NH of Val$^8$ and between the $\alpha$H of Glu$^{10}$ and the NH of Lys$^{12}$ (Figure 2A) suggested the possible presence of type I $\beta$-turns at two locations: K$^5$EVV$^8$ and P$^9$EKK$^{12}$. For the first turn, the absence of a small $^3J_{\alpha N}$ coupling constant (4–5 Hz) for Glu$^6$, as expected for a perfect or stable type I $\beta$-turn, suggested this $\beta$-turn is in rapid equilibrium with unordered coils or other structures. For the second turn, the V$^8$PEK$^{11}$, rather than P$^9$EKK$^{12}$, is a more likely location, since proline is favoured at the (i + 1) position of $\beta$-turns owing to its $\phi$ of $-60°$. This interpretation is also consistent with the large $^3J_{\alpha N}$ coupling constant for Glu$^{10}$. Interestingly, the presence of a NOE crosspeak between the NH of Val$^8$ and the $\delta$H of Pro$^9$ (Figure 2A) indicated that Val$^8$ is at the junction of two $\beta$-turns.

To visualize the appearance of turn structure in PEVK peptide, we built molecular models for K$^5$EVVPEK$^{11}$ using $\phi$ and $\psi$ appropriate for an ideal type I turn (K$^5$EVV$^8$ and V$^8$PEK$^{11}$). The inter-atom distance within the model was consistent with the experimental NOE data (Figure 2C). For example, the amide proton distances between Glu$^6$ and Val$^7$, Val$^7$ and Val$^8$, Glu$^{10}$ and Lys$^{11}$ were 3.32, 2.30 and 2.34 Å respectively. It is worth noting that these two type I $\beta$-turns overlap at Val$^8$ to give an S-shaped structure (Figure 2D).

The decrease of PPII content and the formation of more compact structure in TFE were also evident in the NMR data. First, the appearance of NH-NH(i, i + 1) NOEs, which are characteristically absent in PPII, indicated the conversion of PPII into other more compact structures. Secondly, the decrease of the intensity ratios of $\alpha$H-NH(i, i + 1) and NH-NH(i, i + 1), as well as $\alpha$H-NH(i, i + 1)/$\alpha$H-NH(i, i) also revealed such a conversion. For example, the $\alpha$H-NH(i, i + 1)/$\alpha$H-NH(i, i) ratio for Val$^{15}$ fell from 11.3 [23] to 7.6 in 80 % TFE (Figure 2C), indicating the conversion of extended PPII into a more compact $\beta$-turn or unordered coil in the region A$^{13}$PVAPP$^{18}$ in 80 % TFE.

Elsewhere in the PR peptide, the presence of amide NOE crosspeaks for Val$^{15}$-Ala$^{16}$, Lys$^{19}$-Lys$^{20}$, Glu$^{22}$-Val$^{23}$ and Val$^{26}$-Lys$^{27}$ (Figure 2B) suggested that $\beta$-turns might exist in these regions. However, the absence of $\alpha$H-NH(i, i + 2) NOEs and very weak NOEs between the $\delta$H of Pro$^{14}$, Pro$^{25}$ and the NH of Val$^{15}$ and Val$^{26}$ respectively (Figure 2A) indicated a deviation from perfect or stable turns. Again, other unordered structures may coexist in this region.

It should be noted that NMR data reflect a population-weighted mean of the contributing conformations along the peptide, without indicating the relative content of each conformation. In contrast, CD provides overall relative content of multiple conformations, without specifying the number and locations of each states.

The conversion of PPII helix into $\beta$-turn in low-polarity solvents may be facilitated by the abundance of proline residues that are found frequently in turn structures [37]. Studies on tritrypticin [38] and the C-terminal domain of the RNA polymerase II [39] revealed the coexistence of PPII and $\beta$-turn in solution. Interestingly, multiple $\beta$-turns are capable of forming $\beta$-turn helices [40], raising the possibility of such novel helices in PEVK segments, especially in a less polar environment.

### Ionic strength affects salt bridges

To explore the influence of ionic strength on the conformation of the PEVK peptide (PR), CD spectra were recorded with the addition of 50, 100, 150 and 200 mM KCl (Figure 3A). Altering the concentration of KCl had no effect on the spectra, indicating no change in peptide conformation. Interestingly, NMR data showed that, although the majority of peaks remained unchanged, the Lys$^{12}$ crosspeak is shifted and weakened significantly in 100 mM KCl (Figures 3B and 3C). Such specific ionic-strength sensitivity indicates that Lys$^{12}$, which localizes to the flexible region of the PR peptide, is involved in a salt bridge with anionic side chains. It is therefore probable that ionic strength alters the side-chain conformation of PEVK peptides.

### Urea increases PPII content

It was interesting to note that urea treatment (> 6 M) of polyproline caused a continued increase in intensity of both positive (approx. 229 nm) and negative (approx. 206 nm) bands (Figure 4A). The presence of an isodichroic point at 218 nm suggested an equilibrium of unordered and PPII conformations.

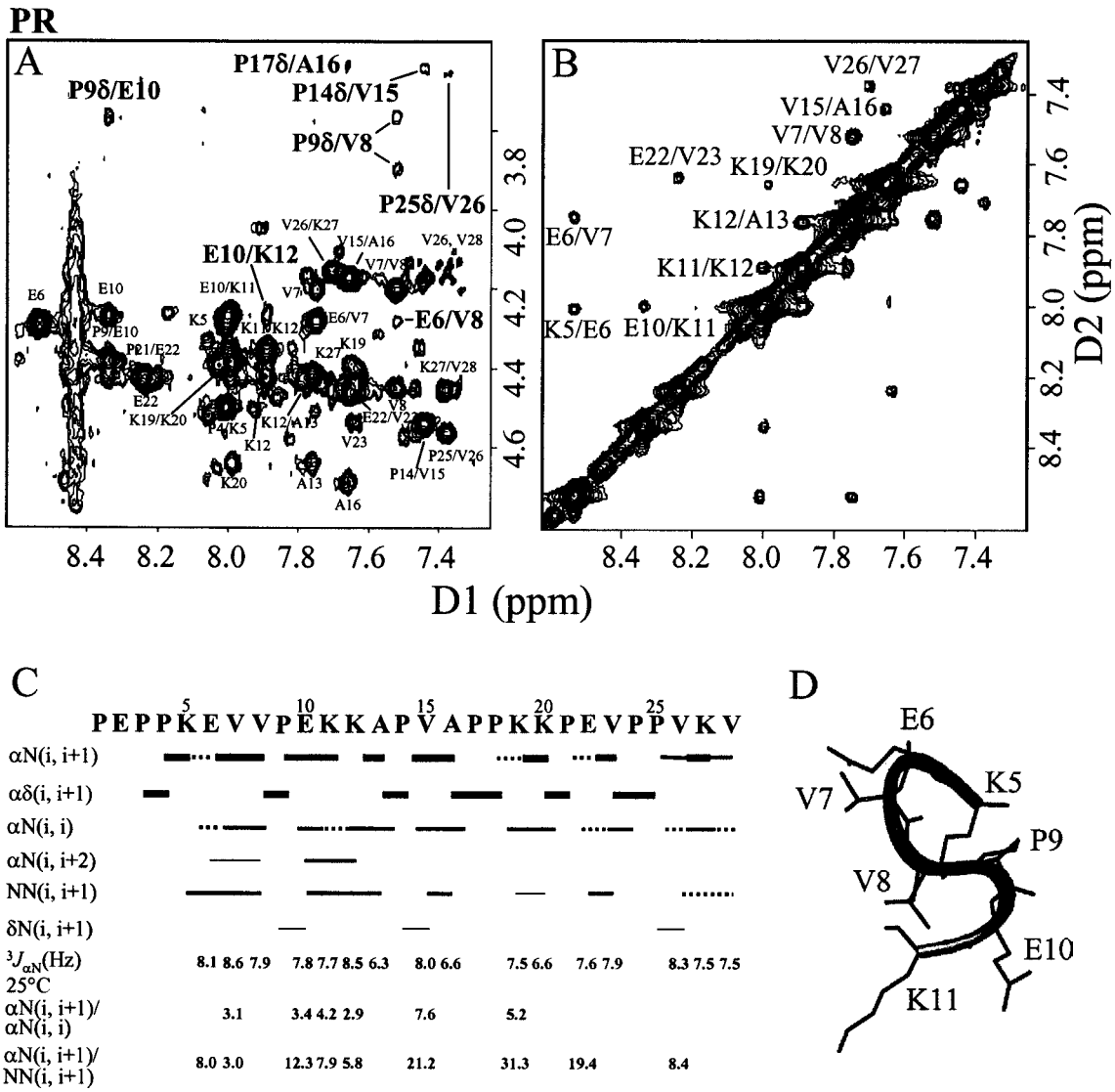


**Figure 2 Two-dimensional NMR of PR**

PR (13 mg/ml, in 80% TFE and 10 mM sodium phosphate, pH 6.9) at 25 °C. (**A**) Expanded $\alpha$H-NH region of NOESY. Crosspeaks corresponding to $\beta$-turn structures are labelled in bold. (**B**) Expanded amide region of NOESY. The assignments are indicated by the sequential number of the corresponding amino acid of PR. (**C**) NMR parameters, including sequential NOEs for PR and the $^3J$ coupling constants at 25 °C. The relative intensities of NOEs are reflected by the thickness of the lines. When an unambiguous assignment was not possible due to spectral overlap, the NOEs were drawn with dots. The intensity ratios of $\alpha$N(i, i + 1)/$\alpha$N(i, i) and $\alpha$N(i, i + 1)/NN(i, i + 1) are also shown for non-overlapping residues. (**D**) Molecular model for $K^5$EVVPE$K^{11}$ using $\phi_{i+1} = -60°$, $\psi_{i+1} = -30°$, $\phi_{i+2} = -90°$ and $\psi_{i+2} = 0°$, appropriate for an ideal type I $\beta$-turn. The whole molecule was energy minimized and labelled with corresponding amino acid residues and their sequential number.

The CD spectra of PR, PR1, PR2 and PR3 peptides in urea at concentrations > 6 M showed the same trend as polyproline in urea (Figure 4B), i.e. more positive above 212 nm and more negative below this wavelength, indicating the presence of PPII conformation. Greater changes were observed with PR2 and PR than PR1 and PR3, indicating higher contents of PPII in the first two peptides. Thus PPII content is enhanced by high concentration of urea, contrary to the urea-induced unfolding of globular protein conformations.

### *Trans*- and *cis*-isomers of proline

The CD analysis described above indicated that PPII content decreased with elevation of temperature. Whether it resulted from isomerization of proline residues remained unclear. The presence of stable conformers of PEVK modules was first demonstrated by the resolution of two peaks of highly purified PR peptide at 4 °C by reverse-phase chromatography (A. Sinz, K. Ma and K.Wang, unpublished work). This observation suggested the presence of *cis*- and *trans*-proline isomers as the basis of such stable conformers. Careful examination of NMR TOCSY and NOESY (ROESY) spectra of PEVK peptides in aqueous solution indicated the presence of one or more minor crosspeaks in addition to the major crosspeaks [23], revealing the presence of minor conformers of PEVK peptides. Further NMR analysis was therefore carried out to elucidate these conformers.

The sequential assignments of PR2 and PR3 were established according to their short- and medium-range NOEs using ROESY spectra. For PR3 (9-mer), nine residues were identified with non-degenerate proton resonances that existed alternately in a major (strong resonance) and a minor (weak resonance) conformation. These included N-terminal residue $Lys^{20}$, $Glu^{22}$, three valine

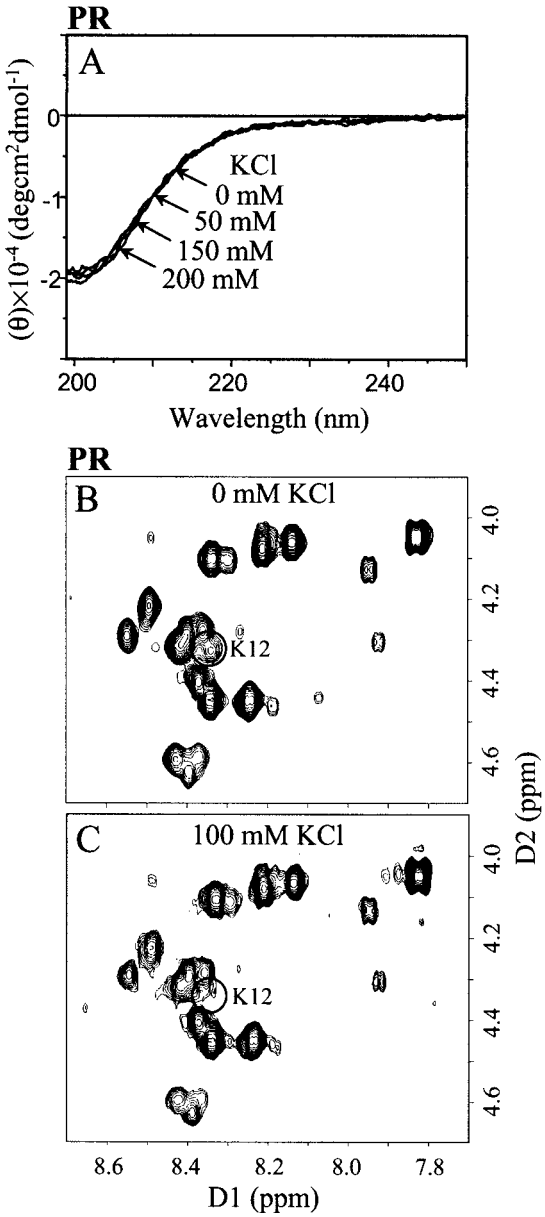


**Figure 3 Ionic-strength titration of PR by CD and NMR**

(**A**) CD spectra of PR (0.06 mg/ml) in 10 mM potassium phosphate, pH 7, with 0, 50, 150 or 200 mM KCl. (**B**) and (**C**) Expanded TOCSY $\alpha$N-NN regions of PR (13 mg/ml) with 0 mM KCl (**B**) or 100 mM KCl (**C**). Changes at Lys[12] are labelled with circles.

residues and Lys[27], some of which showed sequential NOEs to each other in the minor conformation. Three proline residues (Pro[21], Pro[24] and Pro[25]) were found to exhibit non-degenerate intra-residue crosspeaks. A large $\alpha$H chemical shift difference ($>0.2$ p.p.m.) was observed for the proton resonance of one (Pro[24]) of these three proline residues between major and minor conformation. Similarly, for PR2 (12-mer), in addition to the expected 12 residues of the major conformation, seven residues of weaker intensity resonance were also observed. They were assigned to Glu[10], Ala[13], Ala[16], Val[15], and Pro[14], Pro[17] and Pro[18]). Of these three proline residues, Pro[14] and Pro[17] were found to exhibit a large $\alpha$H chemical shift difference ($>0.2$ p.p.m.) between major and minor conformations.

The most probable cause of the minor conformation is the isomerization around one or more of the peptide bonds preceding

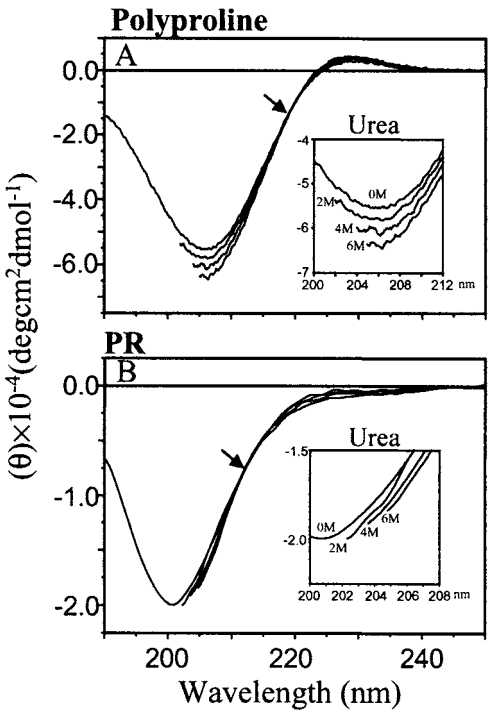


**Figure 4 Polyproline and PR in urea**

(**A**) and (**B**) CD spectra of polyproline (2.0 mg/ml) and PR (1.1 mg/ml) in 10 mM potassium phosphate, pH 7.0, at 0, 2, 4 and 6 M urea. Arrows indicate the isodichroic points. The enlarged regions (200–212 nm) are shown in each inset. Absorption of high concentrations of urea obscured spectra below 200 nm.

the proline residues. Proline *cis*- and *trans*-isomers can be differentiated based on interproton distances between the $\alpha$H of the preceding residues and the proline $\alpha$H and $\delta$H protons. A short distance (NOE signal) between the $\alpha$H of the preceding residue and the $\delta$H of the proline is diagnostic for the *trans*-configuration, whereas a short distance (NOE signal) between the $\alpha$H of the preceding residues and the $\alpha$H of the proline is diagnostic for the *cis*-configuration. In the $^2H_2O$ ROESY spectra, the major observation of the $\alpha\delta$(i, i + 1) NOE crosspeaks for both PR2 and PR3 indicated that all proline residues adopted mainly a *trans*-disposition, consistent with the PPII conformation. However, the crosspeaks between the following pairs were observed: $\alpha$H of Ala[13] and $\alpha$H of Pro[14], $\alpha$H of Ala[16] and $\alpha$H of Pro[17], and $\alpha$H of Pro[17] and $\delta$H of Pro[18] (for PR2; Figure 5A), $\alpha$H of Val[23] and $\alpha$H of Pro[24], and $\alpha$H of Pro[24] and $\delta$H of Pro[25] (for PR3; Figure 5B). These data strongly suggested that Pro[14], Pro[17] in PR2 and Pro[24] in PR3 also adopted a *cis*-conformation in the minor conformers, whereas Pro[18] in PR2 and Pro[25] in PR3 were *trans* in both major and minor conformations. This provides strong experimental evidence that the minor isomers arise from *cis*-proline bond at the Ala[13]-Pro[14], Ala[16]-Pro[17] (for PR2) and Val[23]-Pro[24] (for PR3).

In order to determine the relative amounts of the two isomers, the peaks in $^2H_2O$ TOCSY spectra (Figures 5C–5F) were volume-integrated. The relative peak-intensity ratio of minor and major conformations increased slightly with an elevation in temperature from 5 to 35 °C. The peak-intensity ratio only increased by 4 % for PR2 and 2 % for PR3 within the above-mentioned temperature range, which was much smaller than the extent of decrease of PPII estimated by CD (38 % for PR2 and 17 % for PR3; Figures 1E and 1G). No large exchange existed between the

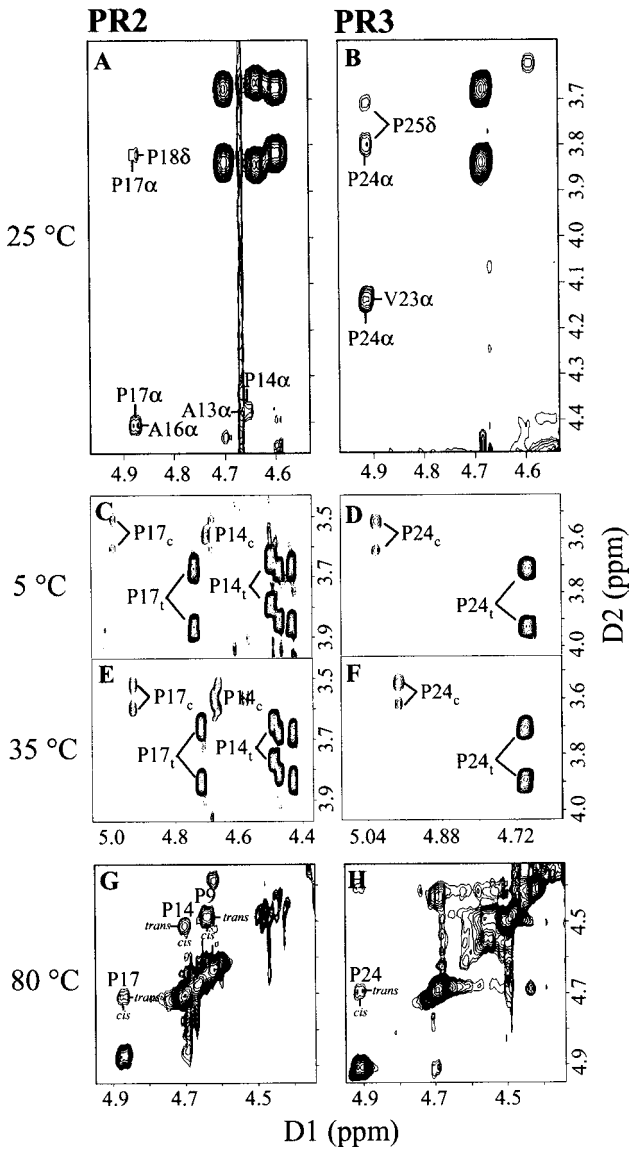


**Figure 5 Two-dimensional NMR of PR2 and PR3 at 5, 25, 35 and 80 °C**

PR2 (9.5 mg/ml) and PR3 (8.3 mg/ml) in 10 mM potassium phosphate, pH 7.0. (**A**) and (**B**) Expanded $\alpha$N-$\alpha$N region of ROESY region for PR2 (**A**) and PR3 (**B**) at 25 °C. (**C**)–(**F**) Expanded $\alpha$N-$\alpha$N region of TOCSY region for PR2 [(**C**) and (**E**)] or PR3 [(**D**) and (**F**)] at 5 °C [(**C**) and (**D**)] or 35 °C [(**E**) and (**F**)]. (**G**) and (**H**) Expanded $\alpha$N-$\alpha$N region of ROESY region for PR2 (**G**) or PR3 (**H**) at 80 °C. All assignments correspond to the sequential number of the amino acid of PR.

*cis*- and *trans*-isomers in PR2 and PR3 within the temperature range 5–35 °C (Figures 5C–5F), suggesting again that the large CD ellipticity change in this temperature range was not due to *trans*-to-*cis* isomerization. The major *trans*-conformation still remained up to 35 °C. The observation that helix-coil transition occurs between 5 and 35 °C without proline isomerization was not unexpected, given the fact that proline *trans*-to-*cis* isomerization is a slow reaction with a free energy of approx. 85 kJ/mol [41]. Indeed, proline isomerization of the Xaa-Pro peptide bond is often catalysed enzymically by peptidyl-prolyl *cis–trans*-isomerases (PPIases) such as cyclophilins, FKBPs (FK506-binding proteins) and parvulins [42].

As the temperature reached 80 °C, most crosspeaks disappeared owing to fast movement of the molecule, except the correlation

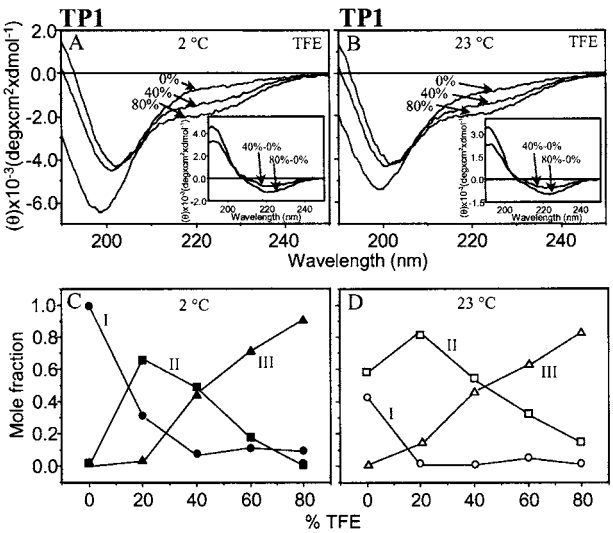


**Figure 6 Conformational states of a 16-module PEVK protein**

CD spectra of TP1 (5 $\mu$M) were recorded at different temperatures and TFE concentrations. (**A**) and (**B**) CD spectra at 2 °C (**A**) and 23 °C (**B**) at 0%, 40% and 80% TFE in 10 mM potassium phosphate, pH 7.0. Inset, difference CD spectra. (**C**) and (**D**) Changes in the relative contents (mole fraction) of conformational states of TP1 in TFE, at 2 °C (**C**) (●, ■, ▲ for component I, II and III respectively) and 23 °C (**D**) (○, □, △ for component I, II and III respectively), under the same conditions as those for (**A**) and (**B**).

within the side chain of glutamic and lysine residues and crosspeaks between $\alpha$H of alanine residues and its $\beta$H. It was noted that the presence of the exchange peaks in ROESY for PR2 and PR3 suggest the occurrence of *trans*-to-*cis* interconversion at high temperature (Figures 5G and 5H). The low amount of *cis*-proline residues and the absence of *trans*-to-*cis* isomerization precluded the absence of right-handed PPI helix within the PEVK peptide in aqueous solution near physiological temperature. Proline isomerization, however does occur at much higher temperatures. The presence of more *cis*-proline conformers at higher temperature has been observed previously [43].

### Conformational interconversion of TP1, a 16-module PEVK protein

To evaluate further whether or not these conformational interconversions are also manifested in PEVK proteins containing multiple modules, we carried out CD measurements on TP1, a 51 kDa expressed protein containing 16 PEVK modules from the human foetal titin PEVK sequence. Changing the ionic strength with the addition of 35, 70, 140, 280 and 560 mM KCl (results not shown) had no effect on the CD spectra of the TP1 protein, indicating that the mean peptide conformation of the PEVK protein was not affected by ionic interactions.

The CD spectra for TP1 protein in increasing amounts of TFE at two different temperatures (2 and 23 °C) indicated major conformational changes (Figures 6A and 6B). The negative band at 199 nm in aqueous solution decreased in intensity and blue-shifted to 203 nm in 40% TFE and further to 204 nm in 80% TFE. The shoulder at 224 nm became more negative with increasing TFE. These changes are consistent with the formation of $\alpha$-helix and/or $\beta$-turn in TFE solution. The CD difference spectra (Figures 6A and 6B, insets) revealed the presence of a type I $\beta$-turn rather than $\alpha$-helix, which has a positive peak at 192 nm and negative bands around 224 nm [34].

The same three components were found to be minimal for the deconvolution of the CD spectra of TP1 in TFE at 2 and 23 °C (Figures 6C and 6D). Estimation of the changes in relative content


**Figure 7 Interconversion of PPII helices, $\beta$-turns and unordered structures of a representative PEVK module (human titin exon 172)**

Three PPII-coil motifs, roughly one every ten residues, are present in aqueous solution at room temperature [23]. The majority of the proline residues are in the *trans* (t) configuration, as required for PPII helices. However *cis* (c) proline residues are detected in small amounts at Ala$^{13}$-Pro$^{14}$, Pro$^{17}$-Pro$^{18}$ and Pro$^{24}$-Pro$^{25}$, revealing the coexistence of a minor conformer without PPII at these positions. The interconversion of three conformational states, PPII helix (PPII), $\beta$-turn ($\beta$T) and unordered coil (U), accounts for all changes detected by CD and NMR. When the temperature is raised, PPII converts into unordered coils, with the helix in PR2 being more resistant. This transition occurs without *trans*-to-*cis* proline isomerization from 5–35 °C. Some proline isomerization does occur at higher temperatures. The module is nearly completely unordered coil above 80 °C. The addition of TFE converts some of the PPII into the unordered coils, and most of the ordered coils into $\beta$-turns, where charged groups are concentrated. Again, no *trans*-to-*cis* isomerization takes place with the addition of TFE. The presence of the chaotrophic agent urea (6 M) induces more PPII. Interestingly, raising the ionic strength does not alter backbone conformations, but does abolish some salt bridges between side chains. Previously, we have demonstrated that $Cu^{2+}$ converts PPII/coil into a $\beta$-turn-like structure at specific sites within the first ten residues [44].

(mole fraction) of each component in the TP1 indicated that 20 % TFE caused the conversion from PPII into coil and $\beta$-turn. Higher TFE concentrations (> 80 %) resulted in a transition from PPII and coil into a type I $\beta$-turn at both 2 and 23 °C (Figures 6C and 6D). The addition of 35, 70, 140, 280 and 560 mM KCl to TP1 in 60 % TFE/buffer solution caused no further spectral changes other than those caused by 60 % TFE (results not shown).

## Malleable conformation and fine-tuning of protein interaction and molecular elasticity

In summary, PEVK conformation is malleable and environmentally sensitive. As shown in Figure 7, the 28-mer PEVK module consists of three PPII-coil motifs, roughly one every ten residues in aqueous solution at room temperature [23]. The majority of the proline residues are in the *trans*-configuration, as required for PPII helices. However a small amount of *cis*-proline residues is detected at Ala$^{13}$-Pro$^{14}$, Pro$^{17}$-Pro$^{18}$ and Pro$^{24}$-Pro$^{25}$, revealing the coexistence of a minor conformer without PPII at these positions. The interconversion of three conformational states, PPII helix, $\beta$-turn and unordered coil, accounts for all changes detected by CD and NMR. When the temperature is raised, PPII converts into unordered coils, with the helix in PR2 being more resistant. This transition occurs without *trans*-to-*cis* proline isomerization from 5 to 35 °C. Some proline isomerization does occur at higher temperatures. The module is nearly completely unordered coil above 80 °C. The addition of TFE converts some of the PPII into unordered structures and most of the unordered structures into type I $\beta$-turns, where charged groups are concentrated. Again, no *trans*-to-*cis* isomerization takes place with the addition of TFE. The presence of the chaotropic agent, urea (6 M), induces more PPII. Interestingly, raising ionic strength does not alter backbone conformations, but does abolish some salt bridges between side chains. We have previously demonstrated that $Cu^{2+}$ converts PPII/unordered coils into a $\beta$-turn structure at specific sites within the first ten residues [44].

The significance of these observations made on one representative module becomes obvious when one considers the wide distribution of the sequence motifs that give rise to the three major conformations in titin PEVK sequences. In human titin PEVK exons, there are 142 PPII motifs (PXPP, XPXXPP, PXXP) and 54 type I $\beta$-turn motifs (KEVV and VPEK), indicating that PPII, turn and coil are likely to be major conformations in various PEVK segments of titin isoforms that were constructed from selected PEVK exons.

The extended and open nature of PPII helices and the factors that influence its dynamic flexibility and accessibility may have important functional roles in the PEVK segment of titin, which is involved in sarcomere assembly and muscle elasticity. PPII helix is a versatile conformation that acts as an intermediate in many conformation transitions, such as $\alpha$-helix $\rightarrow$ $\beta$-sheet [45,46]. This malleability of PPII is unique and allows it to be involved in many protein interactions in unfolded, open and flexible structures [47,48]. More importantly, the responsiveness of PPII to subtle changes in the environment allows protein interactions to be finely tuned by incremental conformational changes, both rapidly and reversibly. For example, the gradual decrease of PPII content in PEVK as the temperature increases is in great contrast with the sharp co-operative 'melting' of globular folded proteins. Our recent study of the interaction of the nebulin SH3 domain with PR and PR2 indicated that the affinity constants are 2–3 times higher at 2 °C than at 22 °C [13]. Such a change may reflect, at least in part, the stabilization of PPII helices at the binding sites (KKAPVAPPK) in PEVK peptides at lower temperatures (Figure 7). The transition from PPII to other conformations in a hydrophobic environment would also be expected to fine-tune or modulate protein interactions. Thus the absence of long-range co-operativity of the PEVK conformations may be an essential attribute of a molecular mechanism that fine-tunes protein interaction. The slow and energetically unfavourable *trans*-to-*cis* isomerization of proline residues may participate in titin regulation at a very different level, perhaps by the participation of either proline isomerases or metal ions that catalyse the isomerization of proline residues [42,44,49].

The effect of ionic strength on the salt-bridge formation among the charged side chains and the resistance of backbone conformation of PEVK modules have significant implications for the understanding of the structural basis of titin PEVK elasticity. As reported elsewhere [50], our recent atomic-force-microscopy studies of the elasticity of TP1 at a single-molecule level indicate that the ion-pairing scheme among the side chains of glutamic and lysine residues, rather than the backbone conformation, plays a dominating role in titin PEVK elasticity. Since the charged groups are concentrated in the coil regions between PPII helices (Figure 7), the ion-pairing effect is greatly amplified by both the high density of side chains as well as the flexibility of the backbone [50].

We thank Mr Gustavo Gutierrez-Cruz for kindly providing TP1 protein and Dr Jeffrey G. Forbes and Dr Patrick C. Nahirney for critically reading this manuscript. We also thank the Cleveland Center for Structural Biology for the use of their NMR spectrometer.

## REFERENCES

1 Wang, K., McClure, J. and Tu, A. (1979) Titin: major myofibrillar components of striated muscle. Proc. Natl. Acad. Sci. U.S.A. **76**, 3698–3702

2 Maruyama, K., Kimura, S., Ohashi, K. and Kuwano, Y. (1981) Connectin, an elastic protein of muscle: identification of "titin" with connectin. J. Biochem. (Tokyo) **89**, 701–709
3 Bang, M. L., Centner, T., Fornoff, F., Geach, A. J., Gotthardt, M., McNabb, M., Witt, C. C., Labeit, D., Gregorio, C. C., Granzier, H. and Labeit, S. (2001) The complete gene sequence of titin, expression of an unusual 700-kDa titin isoform, and its interaction with obscurin identify a novel Z-line to I-band linking system. Circ. Res. **89**, 1065–1072
4 Venter, J. C., Adams, M. D., Myers, E. W., Li, P. W., Mural, R. J., Sutton, G. G., Smith, H. O., Yandell, M., Evans, C. A., Holt, R. A. et al. (2001) The sequence of the human genome. Science **291**, 1304–1351
5 Horowits, R. (1999) The physiological role of titin in striated muscle. Rev. Physiol. Biochem. Pharmacol. **138**, 57–96
6 Wang, K., Forbes, J. G. and Jin, A. J. (2001) Single molecule measurements of titin elasticity. Prog. Biophys. Mol. Biol. **77**, 1–44
7 Young, P., Ferguson, C., Bauelos, S. and Gautel, M. (1998) Molecular structure of the sarcomeric Z-disk: two types of titin interactions lead to an asymmetrical sorting of $\alpha$-actinin. EMBO J. **17**, 1614–1624
8 Labeit, S. and Kolmerer, B. (1995) Titins: giant proteins in charge of muscle ultrastructure and elasticity. Science **270**, 293–296
9 Linke, W. A., Ivemeyer, M., Mundel, P., Stockmeier, M. R. and Kolmerer, B. (1998) Nature of PEVK–titin elasticity in skeletal muscle. Proc. Natl. Acad. Sci. U.S.A. **95**, 8052–8057
10 Freiburg, A., Trombitas, K., Wolfgang, H., Cazorla, O., Fougerousse, F., Centner, T., Kolmerer, B., Witt, C., Beckmann, J. S., Gregorio et al. (2000) Series of exon-skipping events in the elastic spring region of titin as the structural basis for myofibrillar elastic diversity. Circ. Res. **86**, 1114–1121
11 Gutierrez-Cruz, G., Van Heerden, A. and Wang, K. (2001) Modular motif, structural folds and affinity profiles of PEVK segment of human fetal skeletal muscle titin. J. Biol. Chem. **276**, 7442–7449
12 Yamasaki, R., Berri, M., Wu, Y., Trombitas, K., McNabb, M., Kellermayer, M. S., Witt, C., Labeit, D., Labeit, S., Greaser, M. and Granzier, H. (2001) Titin–actin interaction in mouse myocardium: passive tension modulation and its regulation by calcium/S100A1. Biophys. J. **81**, 2297–2313
13 Ma, K. and Wang, K. (2002) Interaction of nebulin SH3 domain with titin PEVK and myopalladin: implications for the signaling and assembly role of titin and nebulin. FEBS Lett. **532**, 273–278
14 Politou, A. S., Spadaccini, R., Joseph, C., Brannetti, B., Guerrini, R., Helmer-Citterich, M., Salvadori, S., Temussi, P. A. and Pastore, A. (2002) The SH3 domain of nebulin binds selectively to type II peptides: theoretical prediction and experimental validation. J. Mol. Biol. **16**, 305–315
15 Labeit, S., Kolmerer, B. and Linke, W. A. (1997) The giant protein titin: emerging roles in physiology and pathophysiology. Circ. Res. **80**, 290–294
16 Bustamante, C., Marko, J. F., Siggia, E. D. and Smith, S. (1994) Entropic elasticity of $\lambda$-phage DNA. Science **265**, 1599–1600
17 Greaser, M. (2001) Identification of new repeating motifs in titin. Proteins **43**, 145–149
18 Wang, M. D., Yin, H., Landick, R., Gelles, J. and Block, S. M. (1997) Stretching DNA with optical tweezers. Biophys. J. **72**, 1335–1346
19 Machado, C. and Andrew, D. J. (2000) D-titin: a giant protein with dual roles in chromosomes and muscles. J. Cell Biol. **151**, 639–651
20 Fukuzawa, A., Shimamura, J., Takemori, S., Kanzawa, N., Yamaguchi, M., Sun, P., Maruyama, K. and Kimura, S. (2001) Invertebrate connectin spans as much as 3.5 $\mu$m in the giant sarcomeres of crayfish claw muscle. EMBO J. **20**, 4826–4835
21 Flaherty, D. B., Gernert, K. M., Shmeleva, N., Tang, X., Mercer, K. B., Borodovsky, M. and Benian, G. M. (2002) Titins in *C. elegans* with unusual features: coiled-coil domains, novel regulation of kinase activity and two new possible elastic regions. J. Mol. Biol. **323**, 533–549
22 Champagne, M. B., Edwards, K. A., Erickson, H. P. and Kiehart, D. P. (2000) *Drosophila* stretchin-MLCK is a novel member of the titin/myosin light chain kinase family. J. Mol. Biol. **300**, 759–777
23 Ma, K., Kan, L. and Wang, K. (2001) Polyproline II helix is a key structural motif of the elastic PEVK segment of titin. Biochemistry **40**, 3427–3438
24 Perczel, A., Hollosi, M., Tusnady, G. and Fasman, G. D. (1991) Convex constraint analysis: a natural deconvolution of circular dichroism curves of proteins. Protein Eng. **4**, 669–679
25 Perczel, A., Park, K. and Fasman, G. D. (1992) Analysis of the circular dichroism spectrum of proteins using the convex constraint algorithm: a practical guide. Anal. Biochem. **203**, 83–93
26 Greenfield, N. J. (1996) Methods to estimate the conformation of proteins and polypeptides from circular dichroism data. Anal. Biochem. **235**, 1–10
27 Sreerama, N. and Woody, R. W. (1994) Poly(pro)II helices in globular proteins: identification and circular dichroic analysis. Biochemistry **33**, 10022–10025
28 Sreerama, N. and Woody, R. W. (1994) Protein secondary structure from circular dichroism spectroscopy: combining variable selection principle and cluster analysis with neural network, ridge regression and self-consistent methods. J. Mol. Biol. **242**, 497–507
29 Sreerama, N. and Woody, R. W. (2000) Estimation of protein secondary structure from circular dichroism spectra: comparison of CONTIN, SELCON, and CDSSTR methods with an expanded reference set. Anal. Biochem. **287**, 252–260
30 Bax, A. and Davis, D. G. (1985) MLEV-17-based two-dimensional homonuclear magnetization transfer spectroscopy. J. Magn. Reson. **65**, 355–360
31 Bax, A. and Davis, D. G. (1985) Practical aspects of two-dimensional transverse NOE spectroscopy. J. Magn. Reson. **63**, 207–215
32 Ronish, E. W. and Krimm, S. (1974) The calculated circular dichroism of polyproline II in the polarizability approximation. Biopolymers **13**, 1635–51
33 Rabanal, F., Ludevid, M. D., Pons, M. and Giralt, E. (1993) CD of proline-rich polypeptides: application to the study of the repetitive domain of maize glutelin-2. Biopolymers **33**, 1019–1028
34 Woody, R. W. (1996) In Circular Dichroism and the Conformational Analysis of Biomolecules (Fasman, G. D., ed.), pp. 25–68, Plenum Press, New York
35 Gierasch, L. M., Deber, C. M., Madison, V., Niu, C.-H. and Blout, E. R. (1981) Conformations of (D-L-Pro-Y)$_2$ cyclic hexapeptides, preferred $\beta$-turn conformers and implications for $\beta$ turns in proteins. Biochemistry **20**, 4730–4738
36 Buck, M. (1998) Trifluoroethanol and colleagues: cosolvents come of age. Recent studies with peptides and proteins. Q. Rev. Biophys. **31**, 297–355
37 Hutchinson, E. G. and Thornton, J. M. (1994) A revised set of potentials for $\beta$-turn formation in proteins. Protein Sci. **3**, 2207–2216
38 Nagpal, S., Gupta, V., Kaur, K. J. and Salunke, D. M. (1999) Structure–function analysis of tritrypticin, an antibacterial peptide of innate immune origin. J. Biol. Chem. **274**, 23296–23304
39 Bienkiewicz, E. A., Moon Woody, A. and Woody, R. W. (2000) Conformation of the RNA polymerase II C-terminal domain: circular dichroism of long and short fragments. J. Mol. Biol. **297**, 119–133
40 Matsushima, N., Creutz, C. E. and Kretsinger, R. H. (1990) Polyproline, $\beta$-turn helices: novel secondary structures proposed for the tandem repeats within rhodopsin, synaptophysin, synexin, gliadin, RNA polymerase II, hordein, and gluten. Proteins **7**, 125–155
41 Mayo, K. H., Parra-Diaz, D., McCarthy, J. B. and Chelberg, M. (1991) Cell adhesion promoting peptide GVKGDKGNPGWPGAP from the collagen type IV triple helix: *cis/trans* proline-induced multiple $^1$H NMR conformations and evidence for a KG/PG multiple turn repeat motif in the all-*trans* proline state. Biochemistry **30**, 8251–8267
42 Gothel, S. F. and Marahiel, M. A. (1999) Peptidyl-prolyl *cis-trans* isomerases, a superfamily of ubiquitous folding catalysts. Cell. Mol. Life Sci. **55**, 423–436
43 McInnes, C., Kay, C. M., Hodges, R. S. and Sykes, B. D. (1994) Conformational differences between *cis* and *trans* proline isomers of a peptide antigen representing the receptor binding domain of *Pseudomonas aeruginosa* as studied by $^1$H-NMR. Biopolymers **34**, 1221–1230
44 Ma, K. and Wang, K. (2003) Binding of copper(II) ions to the polyproline II helices of PEVK modules of the giant elastic protein titin as revealed by ESI-MS, CD and NMR. Biopolymers, in the press
45 Blanch, E. W., Morozova-Roche, L. A., Cochran, D. A., Doig, A. J., Hecht, L. and Barron, L. D. (2000) Is polyproline II helix the killer conformation? A Raman optical activity study of the amyloidogenic prefibrillar intermediate of human lysozyme. J. Mol. Biol. **301**, 553–563
46 Uversky, V. N. (2002) What does it mean to be natively unfolded? Eur. J. Biochem. **269**, 2–12
47 Creamer, T. P. and Campbell, M. N. (2002) Determinants of the polyproline II helix from modeling studies. Adv. Protein Chem. **62**, 263–282
48 Shi, Z., Woody, R. W. and Kallenbach, N. R. (2002) Is polyproline II a major backbone conformation in unfolded proteins? Adv. Protein Chem. **62**, 163–240
49 Cox, C. and Lectka, T. (2000) Synthetic catalysis of amide isomerization. Acc. Chem. Res. **33**, 849–858
50 Forbes, J. G., Jin, A. J., Ma, K. and Wang, K. (2003) Elasticity of the PEVK segment of titin is dominated by sequence-specific charge pairing interactions. Biophys. J. **84**, 140a


Received 13 May 2003/10 June 2003; accepted 20 June 2003
Published as BJ Immediate Publication 20 June 2003, DOI 10.1042/BJ20030702